TEMPERATURE EFFECT ON THE TWO-DIMENSIONAL PHASE TRANSITION KINETICS OF ADENINE ADSORBED AT THE Hg ELECTRODE/AQUEOUS SOLUTION INTERFACE

Claudio FONTANESI[1,*], Roberto ANDREOLI, Luca BENEDETTI, Roberto GIOVANARDI and Paolo FERRARINI

Department of Chemistry, University of Modena and Reggio Emilia, Via Campi 183, 41100 Modena, Italy; e-mail: [1] fontanes@unimo.it

Received January 20, 2003
Accepted April 24, 2003

This work is especially dedicated to Professor Sergio Roffia, on the occasion of his retirement from academic duties. It concerns the molecular electrochemistry, to which Prof. Roffia has fruitfully devoted his research activity and efforts over a long time.

The kinetics of the liquid-like → solid-like 2D phase transition of adenine adsorbed at the Hg/aqueous solution interface is studied. Attention is focused on the effect of temperature on the rate of phase change; an increase in temperature is found to cause a decrease of transition rate.

Keywords: Parallel-perpendicular orientation; 2D phase transitions; Current transients; Capacity transients; Purines; Nucleobases; Electrochemistry; Kinetics; Thermodynamics.

2D phases are formed following the adsorption of a substance on a substrate in various ways: organic compounds adsorbed on electrode surfaces[1–3], gaseous substances adsorbed on ordered or amorphous solid surfaces under ultra high vacuum conditions, insoluble long-chain organic compounds adsorbed at the air/aqueous solution interface[4].

Experimental studies relating to equilibrium properties of these systems indicate the existence of 2D phases of different nature: gas-like (g-l), liquid-like (l-l), solid-like (s-l). The analogy with 3D systems extends to polymorphism, which is also present in 2D condensed phases[5].

The electrochemically induced 2D phase transition of organic molecules adsorbed on electrode surfaces is, in some aspects, peculiar. In that, the electric field present at the interface represents an additional controllable intensive variable which contributes to the determination of the most stable adsorbed phase.

The equilibrium properties of this phenomenon have also been recently studied in detail using different modelistic approaches[1,6,7], following the classic papers by Lorenz and Vetterl[8].

Within this picture, the study of the kinetic aspects associated with 2D phase transitions represents a subject still featuring some unclear aspects.

It is known that, in general, a nucleation and growth mechanism rules the kinetics of 3D phase change, when gas → liquid or liquid → solid transformations are dealt with. For these systems, the study of variation of the rate constant of the phase transition with temperature allows to determine the relevant activation energy, a quantity related to the structure properties of the investigated phases.

Few data are available concerning the kinetics of electrochemically induced 2D phase transitions at different temperatures. Even if some studies report data regarding this effect (in general in a very narrow range of temperature[9]), they are never rationalised in terms of an inverse functional dependence between rate constant and temperature. Moreover, one of more exhaustive analyses of kinetic data, regarding uracil, relates temperature and kinetic parameters still at a phenomenological level[10].

Thus the study of the dependence of the kinetics of these processes on temperature seems still lacking.

The aim of this paper is (i) to study the case of the parallel (l-l) → perpendicular (s-l) 2D phase transition of adenine adsorbed at the Hg/aqueous solution interface, for which it was experimentally found that a temperature increase leads to a slower transformation rate and (ii) to rationalize on physical basis this peculiar temperature effect. (In this context “flat” or “parallel” means a molecule adsorbed with the ring plane parallel to the electrode surface; “perpendicular” indicates an angle of nearly 90° between the two planes.)

EXPERIMENTAL

Aqueous solutions of adenine (Aldrich), pK_a = 4.2, pK_b = 9.8, were prepared with MilliQ Plus reagent-grade water; 1 M NaCl (Carlo Erba R.P.E.) solution was used as a base electrolyte. For all solutions, pH was adjusted and maintained at 7 ± 0.05 by addition of small amounts of concentrated HCl and NaOH (Carlo Erba, R.P.E.), so that the neutral molecule was the main electroactive species. Before each measurement, solutions were deaerated with nitrogen for 15 min and the pH was checked before and after each measurement with an AMEL 347 pH-meter and Ingold HA 405-60-K1 pH-combined electrode. The temperature was kept constant within ± 0.1 K.

All the reported measurements were performed using an AMEL 430 A hanging mercury drop electrode HMDE, with the drop area of 0.0217 cm^2 (reproducibility better than 0.5%);

the auxiliary electrode was a Pt wire and a saturated calomel electrode (SCE) as a reference electrode. All the potentials are referred to SCE.

The AC phase-sensitive polarographic measurements were carried out with an AMEL 471 multipolarograph (alternating voltage with a 10 mV peak-to-peak amplitude). Measurements at 100 and 1000 Hz allowed to exclude any effect of frequency on the discontinuity potentials.

Capacity *vs* time (C/t) transients were recorded using an AMEL 565 Function Generator, Solartron 1286 Electrochemical Interface and a 1250 Frequency Response Analyzer (alternating current with a 5 mV peak-to-peak amplitude and 997 Hz frequency).

Current *vs* time (i/t) transients were recorded using the 565 Function Generator, 555 Potentiostat and 430A hanging mercury drop electrode by AMEL and a Nicolet 310 digital oscilloscope.

During C/t and i/t measurements a mercury drop was formed and kept at the initial potential for 10.4 s; the potential was then switched to its final value.

The whole electrochemical apparatus was controlled by an IBM PS2 computer *via* GPIB and RS232 interfaces for time triggering and data acquisition.

The electrochemical system under study equivalent to a series *RC* circuit, required a careful selection of a suitable potentiostatic control loop bandwidth[11]: the Solartron 1286 type A 600 kHz bandwidth, combined with a 10 μs AMEL 565 low-pass filter were selected. In the worst case, these conditions allowed to set the potential steps on the cell free from oscillations and with a rising time < 5 μs.

Transients presented in this paper have been obtained by the single potential step technique[3]: at constant temperature, the variation of a suitable electric quantity (double-layer capacity or direct current) was recorded after stepping the potential from a value relevant to the parallel (l-l) adsorbed phase to a final value relevant to the perpendicular (s-l) adsorbed phase.

In an attempt to impose identical initial conditions (aiming to compare results obtained at different temperatures), the starting potentials (E_{ini}) have been chosen by 0.1 V more negative with respect to the relevant E_{tr}^{-} and by 0.1 V more positive with respect to the relevant E_{tr}^{+} (tables setting out the transition potentials chosen as a function of temperature are presented) for both C/t and i/t transients. Preliminary studies showed that the transients are scarcely affected by a "reasonable" variation of E_{ini}, as already observed in ref.[3]

RESULTS AND DISCUSSION

Figure 1 shows capacity *vs* potential (C/E) curves for a 6×10^{-3} M adenine in 1 M NaCl aqueous solution, recorded at different temperatures. A range of potentials featuring low and constant value of capacity is present (capacitive "pit") whose amplitude is a function of temperature, due to the 2D phase transition[1]:

$$2\ \text{adenine}_{(\text{ads, l-l})} + \text{adenine}_{(\text{bulk})} \rightarrow 3\ \text{adenine}_{(\text{ads, s-l})}\ . \qquad (1)$$

Examples of current and capacitive transients at a constant temperature are shown in Figs 2a and 2b. Here i/t transients are characterized by an ini-

tial decay due to the double layer charging. The subsequent peak is a current flow induced by the variation of capacity associated with the (l-l) → (s-l) 2D phase transition of the adsorbed molecules. Their integration, $\int_{t_0}^{t} i_{dc}\,dt = q_t$ (where i_{dc} is the current and t the time), yields sigmoidal charge *vs* time (q_t/t) curves; this result suggests that the phase transition kinetics is governed by a nucleation and growth mechanism[3]. Transients i/t were recorded at 283, 288 and 293 K and start only from more negative potential values with respect to the capacitive pit because higher temperatures and initial potential values more positive with respect to the "pit" produced a too noisy current signal.

Transients C/t (recorded at 283, 288, 293, 298 and 303 K) present a sigmoidal time dependence, which is again typical of a kinetic process controlled by a nucleation and growth mechanism[2,12]. They are transformed into surface coverage *vs* time (θ_t/t) curves defining

$$\theta_t = (C_0 - C_t) / (C_0 - C_\infty)\,, \qquad (2)$$

where C_0, C_t and C_∞ are the initial, the intermediate at the time t and the final capacity values, θ_t is the surface coverage as a function of time, $0 < \theta_t < 1$.

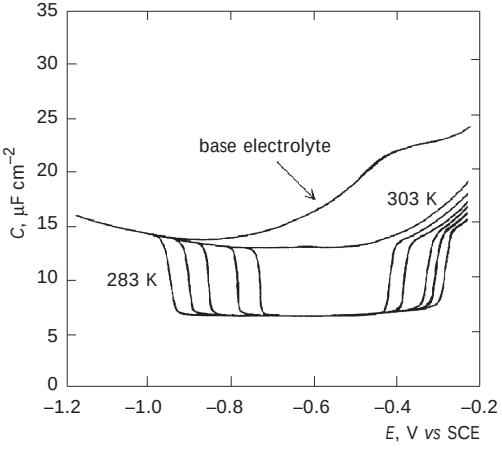

FIG. 1

Interfacial capacity (C) *vs* potential (E) curves, 6×10^{-3} M adenine in 1 M NaCl aqueous solution, pH 7, recorded at temperatures 283, 288, 293, 298, 303 and 308 K. Each curve combines two independently recorded scans both starting from –0.550 V *vs* SCE, one scan to more positive potentials, the other scan to more negative potentials. Scan rate 10 mV s^{-1}, 1000 Hz, 10 mV peak-to-peak amplitude

As proposed by Retter[13], the θ_t/t transients were fitted according to the Avrami equation[14]

$$\theta_t = 1 - \exp(-bt^m), \qquad (3)$$

where t is the time, b is the global kinetic rate constant (determined by the $K_g K_n$ product of the growth and the nucleation rate constants, respectively)

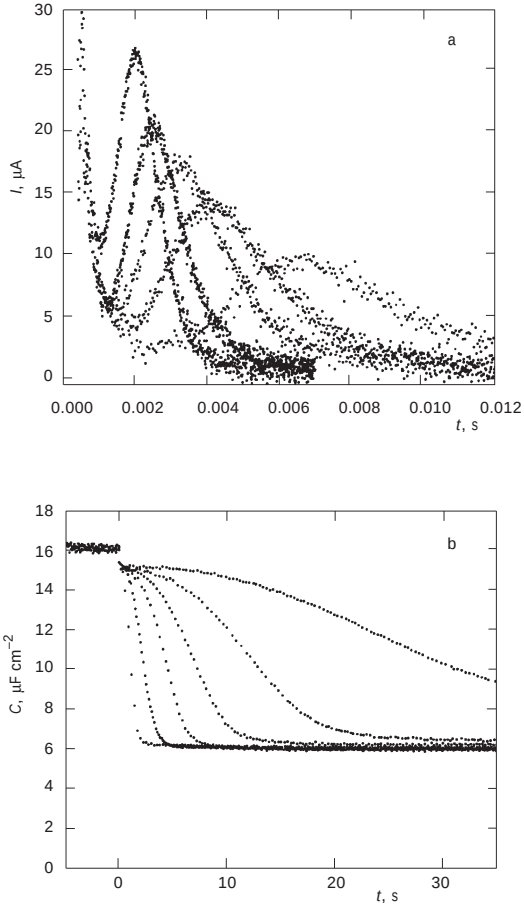

FIG. 2

a Current (I) transients following a single potential step. E_{ini} = –1.025 V *vs* SCE. The final potentials are (from right to left) –0.790, –0.800, –0.820, –0.840 and –0.860 V *vs* SCE, T = 283 K. b Capacity (C) transients following a single potential step. E_{ini} = –1.025 V *vs* SCE. The final potentials are (from right to left) –0.923, –0.918, –0.913, –0.908 and –0.903 V *vs* SCE, T = 283 K

and m = 1, 2, 3, 4, is a parameter determined by the kinetic mechanism. For the present 2D system m = 2 should indicate an instantaneous nucleation and m = 3 should indicate a progressive nucleation mechanism[14]. Actually, in the $0.1 < \theta_t < 0.9$ range, an effective fit of the experimental data can be obtained. Inspection of the obtained data fitting Eq. (*3*) shows that, at a fixed temperature, the dependence of ln b as a function of E_{fin} follows a loose parabolic pattern (Fig. 3a), and that m values are comprised between 2 and 3 (see, as an example, the whole set of data reported in Tables I and II

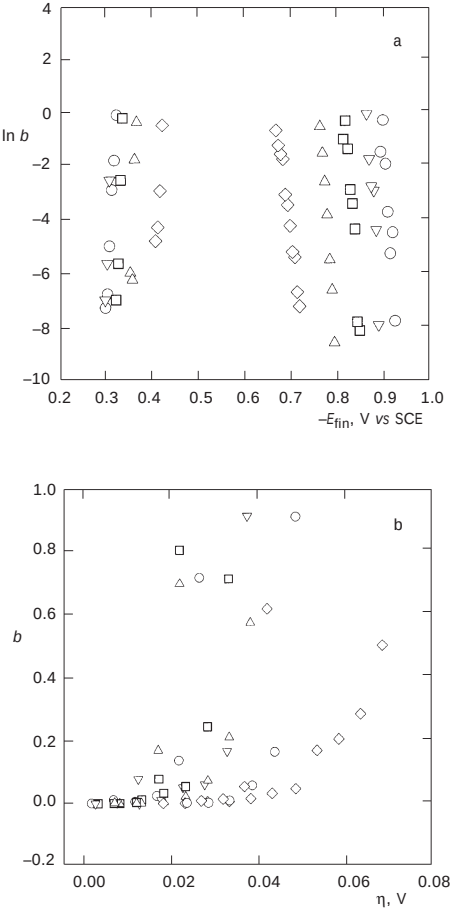

FIG. 3

a Logarithm of the Avrami rate constant b *vs* final potential value (E_{fin}). b Global Avrami rate constant b *vs* η ($\eta = |E_{tr}^{+\text{ or }-} - E_{fin}|$) at various temperatures T, K: ◇ 303, Δ 298, □ 293, ∇ 288 and ○ 283

for two different temperatures and with different experimental conditions (E_{ini}, E_{fin}).

An increase in temperature causes a decrease in the magnitude of b, as can be found comparing b values interpolated for a fixed value of E_{fin}. As expected, the pattern of b as a function of η (η = $|E_{tr}^{+\text{ or }-} - E_{fin}|$) shows the correct trend, as $b \to 0$ when $\eta \to 0$ (Fig. 3b). Note that the straightforward application of the Arrhenius relation in its usual form, $b_{(E_{fin} = \text{const})}$ = const exp ($-E^{\#}/RT$), yields negative values of the activation energy[15]. Nevertheless, the m values not univocally defined (2 or 3) indicate some sort of inadequacy in the application of the Avrami model to the present situation (see Tables I and II).

The Avrami b parameter is not a true rate constant, because the corresponding $d\theta/dt$ function still depends on both time and θ. The following differential equation has also been used to fit C/t transients, $d\theta/dt = K(1 - \theta)\theta^{(1-n)/n}$, where n is an adjustable parameter and K is a true rate constant. In fact, the

TABLE I
Avrami and Liquori–Tripiciano parameters from C/t transients at T = 283 K

E_{fin} –V *vs* SCE	m	ln b	τ_1, s	τ_2, s
		E_{ini}^{-} = –1.025 V *vs* SCE		
0.9233	2.0	–7.797	347.4	19.942
0.9183	2.5	–4.519	144.8	5.0134
0.9133	2.3	–5.292	118.2	3.1964
0.9083	2.3	–3.765	51.37	1.6480
0.9032	2.3	–2.001	17.51	0.9366
0.8984	2.2	–0.338	6.852	0.4192
0.8930	2.0	+1.548	2.900	0.2061
		E_{ini}^{+} = –0.175 V *vs* SCE		
0.2986	2.5	–7.271	177.6	5.533
0.3035	2.7	–6.776	82.66	3.260
0.3084	2.5	–4.963	51.86	2.326
0.3136	2.2	–2.899	27.22	1.270
0.3187	2.8	–1.819	10.08	0.558
0.3236	2.4	+0.099	6.324	0.314

fit of the experimental C/t curves with this equation yields K values which are different in magnitude, from the corresponding b values, but the ordering with respect to temperature and to E_{fin} remains the same.

Thus, the autocatalytic Liquori–Tripiciano relaxation model, an approach developed within the framework of thermodynamics of irreversible processes[16], has been used to analyze C/t transients. In this case, the underlying "driving force" of the process is assumed to be the reaction affinity, A, $A = -\sum_i \nu_i \mu_i$, where ν_i and μ_i refer to the species involved in the phase transition process as indicated in Eq. (*1*). This approach is characterized by the drawback of being independent of the structure of the system under study. Thus its application, even if it does not produce any further structure insight, assumes that the rate determining steps are two competitive processes of different nature, allowing to determine the absolute proper relaxation times of each process (*i.e.*, the reciprocal of the rate constants).

For sigmoidal shaped transients, the autocatalytic growth model has to be applied[17]. (The autocatalytic approach in the rationalization of interfacial 2D condensation kinetics was pioneered by Michailik, even though by using a different mathematical formalism[18].)

TABLE II
Avrami and Liquori–Tripiciano parameters from C/t transients at T = 298 K

E_{fin} –V *vs* SCE	m	ln b	τ_1, s	τ_2, s
		E^-_{ini} = –0.900 V *vs* SCE		
0.7919	2.5	–8.592	253.1	9.956
0.7869	2.6	–6.638	128.8	4.140
0.7818	2.7	–5.492	61.33	2.250
0.7768	2.5	–3.851	34.60	1.409
0.7717	2.5	–2.625	33.82	0.861
0.7668	2.6	–1.563	23.31	0.545
0.7619	2.4	–0.559	8.755	0.433
		E^+_{ini} = –0.245 V *vs* SCE		
0.3519	1.9	–5.956	148.2	12.31
0.3570	3.6	–6.228	134.7	1.250
0.3620	3.1	–1.779	11.16	0.505
0.3670	3.0	+0.364	9.344	0.247

$$\theta_t = \frac{1 - \exp(-t / \tau_1)}{1 - \exp(-t / \tau_1) + \exp(-t / \tau_2)}, \qquad (4)$$

where τ_1 and τ_2 are the relaxation times relevant to two competitive processes ruling the global kinetics. In this specific case it seems reasonable to consider τ_1 and τ_2 related to K_n and K_g. Thus, the $\tau_1 \tau_2$ product should be proportional to b (ref.[3]). In fact, the plot of the Avrami rate constant b as a function of $(\tau_1 \tau_2)^{-1}$ results in a straight line passing virtually through the origin $b = 0.009 + 1.94(\tau_1 \tau_2)^{-1}$, $r = 0.94$ (Fig. 4).

Again, once E_{fin} fixed, for both τ_1 and τ_2 an increase in temperature yields larger relaxation times, indicating that an increase in temperature causes a decrease in the global phase transition rate.

Finally, once the temperature fixed, a value of E_{fin} can be determined which corresponds to a maximum in the phase transition rate, as shown in Fig. 5, where ln $t_{1/2}$ values are plotted as a function of E_{fin} and of temperature ($t_{1/2}$ is the half-transition time, $\theta_{t_{1/2}} = 0.5$). At fixed temperature, a maximum in the phase transition rate as a function of E_{fin} can be roughly estimated (the lowest value of $t_{1/2}$), $t_{1/2}^{min}$, which corresponds to the maxima of each constant temperature curve in Fig. 5. It is evident that an increase in temperature causes an increase in $t_{1/2}^{min}$ (*i.e.*, a decrease in the phase transition rate).

The continuity observed in Fig. 5, when connecting the ln $t_{1/2}$ values concerning transients recorded in a large range of completion times and

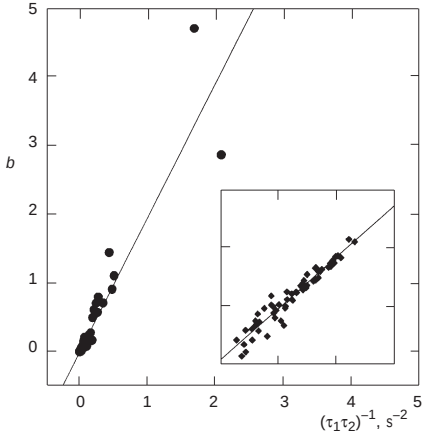

FIG. 4

Avrami rate constant b *vs* the inverse of the Liquori–Tripiciano relaxation times product $\tau_1 \tau_2$. The inset shows the same data represented on a log–log plane

even using two different experimental strategies (C/t and i/t) and the related instrumental set-up, results in a further indication that the nature of the kinetic mechanism of the phase transition remains the same under the investigated conditions.

The effect of temperature on the kinetics of the process can be rationalized taking into account that the Gibbs energy variation (ΔG) of the phase transition process can be considered a function of the radius (r) of the growing phase. In particular, the early stages of the formation of the ordered phase involve a positive and increasing ΔG value as a function of r (refs[2,16]). So, in the case of a 2D system

$$\Delta G = (2\pi\varepsilon)r + (\pi\Delta\tilde{\mu}_{PT} / S)r^2, \qquad (5)$$

where r is the radius of the cluster (assumed circular for the sake of simplicity), ε is the line tension, S the surface occupied by a mole of the cluster (perpendicular orientation), $\pi\Delta\tilde{\mu}_{PT}$ is the molar Gibbs free energy variation associated with the phase transition process.

In Eq. (5) the $2\pi\varepsilon$ term is always positive, whilst the $\pi\Delta\tilde{\mu}_{PT} / S$ term is negative, as the growth of the ordered phase implies $\Delta\tilde{\mu}_{PT} < 0$. Consequently, ΔG, as a function of r, shows a positive maximum when $(\partial\Delta G / \partial r)_{r^\#} = 0$. The

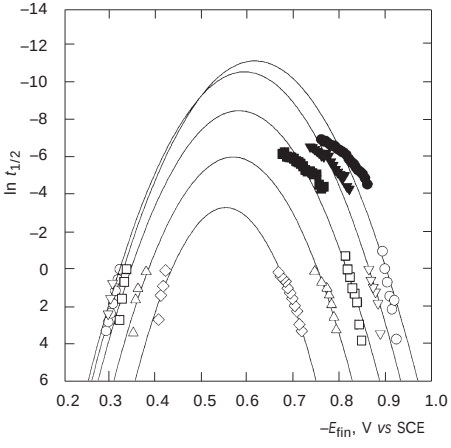

FIG. 5

Logarithm of the half-transition time ($t_{1/2}$, s) *vs* the final potential (E_{fin}) at various temperatures T, K: ◇ 303, Δ 298, □ 293, ∇ 288 and ○ 283. Capacitive transients, empty symbols; current transients, full symbols

relevant cluster radius is $r^{\#} = -S\varepsilon/\Delta\tilde{\mu}_{PT}$ and the corresponding activation Gibbs energy, $\Delta G^{\#}$, results

$$\Delta G^{\#} = -\pi S\varepsilon^2/\Delta\tilde{\mu}_{PT}. \qquad (6)$$

Steady state growth is attained when $r > 2r^{\#}$, a condition which implies $\Delta G < 0$.

The nucleation rate is related to the activation energy $\Delta G^{\#}$ (refs[3,19])

$$J = Z\beta n_1 \exp(-\Delta G^{\#} / KT), \qquad (7)$$

where J is the nucleation rate, Z is the Zeldovich factor, n_1 the initial concentration of adsorbed non-clustered molecules, β is the impingement flux of molecules on the nucleus edge. Combining Eqs (*6*) and (*7*) yields

$$J = Z\beta n_1 \exp(\pi S\varepsilon^2 / \Delta\tilde{\mu}_{PT} KT). \qquad (8)$$

In the case of the 2D phase transition of adenine, the functional dependence of $\Delta\tilde{\mu}_{PT}$ on both the potential and temperature is known[1]. With $C = 6 \times 10^{-4}$ M and for $E_{fin} = -0.5$ V (a value close to the point of zero charge of the base electrolyte), $\Delta\tilde{\mu}_{PT} = -41\,263 + 130T$. Note that, $\Delta\tilde{\mu}_{PT}$ is a negative quantity which becomes smaller, in absolute value, as temperature increases and that the positive temperature coefficient (+130 J mol^{-1} K^{-1}) is the phase transition entropy change[1].

The perpendicular orientation implies that $S = 240 \times 10^3$ m^2 mol^{-1}, while the line tension $\varepsilon = 9.4 \times 10^{-12}$ J m^{-1} (ref.[3]). Thus Eq. (*8*) results, $J = Z\beta n_1 \exp[4.84 \times 10^6/(-41\,263T + 130T^2)]$. Considering Z, β and n_1 independent of temperature implies that J has a maximum for $T = 158$ K (which is a purely theoretical value). Moreover, J is a monotonically decreasing function of temperature in the range of temperatures here investigated. This result is in accordance with the arguments proposed by Retter starting from a lattice gas model[20].

In conclusion, on qualitative grounds, the decrease in J with temperature given by Eq. (*8*), agrees well with experimental results concerning $t_{1/2}$ values. Moreover, on quantitative grounds, the ln $t_{1/2}$ *vs* $1/\Delta\tilde{\mu}_{PT}$ plot is almost linear, featuring the experimentally found dependence of $t_{1/2}$ on tempera-

ture. An increase in temperature, at fixed potential, shifts $1/\Delta\tilde{\mu}_{PT}$ to a more negative value (Fig. 6).

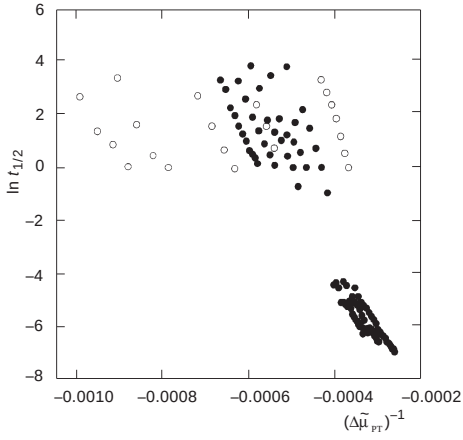

FIG. 6
Logarithm of the half-transition time ($t_{1/2}$, s) *vs* the inverse of the chemical potential variation of the phase transition ($\Delta\tilde{\mu}_{PT}$, kJ mol^{-1}). Full symbols, transients with a value of E_{ini} more negative (anodic) with respect to the potential of the "pit" discontinuity; empty symbols, transients with a value of E_{ini} more positive (cathodic) with respect to the potential of the "pit" discontinuity

Professor Ulderico Segre is kindly acknowledged for helpful discussions. Economical support from the Ministero della Ricerca Scientifica e Tecnologica, COFIN2002 (Responsabile Nazionale Prof. R. Guidelli, Sistemi elettrochimici innovativi: nanostrutture, sistemi di interesse biologico, processi ecocompatibili) Roma, is gratefully acknowledged.

REFERENCES

1. Fontanesi C.: *J. Chem. Soc., Faraday Trans.* **1994**, *90*, 2925.
2. a) de Levie R.: *Chem. Rev. (Washington, D. C.)* **1988**, *88*, 599; b) de Levie R.: *Adv. Electrochem. Electrochem. Eng.* **1985**, *13*, 1.
3. a) Buess-Herman C.: *Adsorption of Molecules at Metal Electrodes*, Chap. 2. VCH Publishers, New York 1992; b) Buess-Herman C.: *Prog. Surf. Sci.* **1994**, *46*, 335.
4. Chan M. H. W.: *Phase Transition in Surface Films 2*, Chap. 1. Plenum Press, New York 1991.
5. Glazer M. A., Clark N. A.: *Adv. Chem. Phys.* **1993**, *83*, 543.
6. Sridharan R., De Levie R., Rangarajan S. K.: *Chem. Phys. Lett.* **1987**, *142*, 43.
7. Kharkats Y. I., Retter U.: *J. Electroanal. Chem.* **1990**, *287*, 363.
8. a) Lorenz W.: *Z. Electrochem.* **1958**, *62*, 192; b) Vetterl V.: *Collect. Czech. Chem. Commun.* **1966**, *31*, 2105.
9. Buess-Herman C., Franck C., Gierst L.: *Electrochim. Acta* **1986**, *31*, 965.

10. Wandlowski T.: *J. Electroanal. Chem. Interfacial Electrochem.* **1990**, *293*, 219.
11. *1286 Electrochemical Interface, Operating Manual*, Chap. 9. Solartron Instruments, Farnborough 1984.
12. Benedetti L., Borsari M., Gavioli G., Fontanesi C.: *J. Electroanal. Chem. Interfacial Electrochem.* **1990**, *279*, 321.
13. Retter U.: *J. Electroanal. Chem. Interfacial Electrochem.* **1980**, *106*, 371.
14. Avrami M.: *J. Chem. Phys.* **1941**, *9*, 177.
15. Borg R. J., Dienes G. J.: *The Physical Chemistry of Solids*, Chap. 5. Academic Press, Boston 1992.
16. Prigogine I.: *Introduction to Thermodynamics of Irreversible Processes*. C. C. Thomas Publisher, Springfield 1955.
17. Liquori A. M., Monroy A., Parisi E., Tripiciano A.: *Differentiation (Berlin)* **1981**, *20*, 174.
18. Michailik Y. V., Damaskin B. B.: *Elektrokhimiya* **1979**, *15*, 478.
19. a) Retter U.: *J. Electroanal. Chem. Interfacial Electrochem.* **1990**, *296*, 445; b) Donner C., Baumgartel H., Pohlmann L., Retter U., Phillip R.: *Ber. Bunsen–Ges. Phys. Chem.* **1996**, *100*, 403.
20. Retter U.: *J. Electroanal. Chem.* **1993**, *349*, 41.